HHS Public Access

Author manuscript

Clin Cancer Res. Author manuscript; available in PMC 2024 July 05.

Published in final edited form as:

Clin Cancer Res. 2023 July 05; 29(13): 2435–2444. doi:10.1158/1078-0432.CCR-23-0118.

Phase I Study of SYNB1891, an Engineered *E. coli* Nissle Strain Expressing STING Agonist, with and without Atezolizumab in Advanced Malignancies

Jason J. Luke[1], **Sarina A. Piha-Paul**[2], **Theresa Medina**[3], **Claire F. Verschraegen**[4], **Mary Varterasian**[5], **Aoife M. Brennan**[6], **Richard J. Riese**[6], **Anna Sokolovska**[6], **James Strauss**[7], **David L. Hava**[6], **Filip Janku**[2]

[1]UPMC Hillman Cancer Center, Pittsburgh, Pennsylvania.

[2]University of Texas, MD Anderson Cancer Center, Houston, Texas.

[3]University of Colorado School of Medicine, Aurora, Colorado.

[4]Ohio State University Comprehensive Cancer Center, Columbus, Ohio.

[5]Ann Arbor Drug Safety, LLC, Ann Arbor, Michigan.

[6]Synlogic Inc., Cambridge, Massachusetts.

[7]Mary Crowley Cancer Research, Dallas, Texas.

Abstract

Purpose: SYNB1891 is a live, modified strain of the probiotic *Escherichia coli* Nissle 1917 (EcN) engineered to produce cyclic dinucleotides under hypoxia, leading to STimulator of Interferon Genes (STING) activation in phagocytic antigen-presenting cells in tumors and activating complementary innate immune pathways.

Patients and Methods: This first-in-human study (NCT04167137) enrolled participants with refractory advanced cancers to receive repeat intratumoral injections of SYNB1891 either alone or in combination with atezolizumab, with the primary objective of evaluating the safety and tolerability of both regimens.

Results: Twenty-four participants received monotherapy across six cohorts, and 8 participants received combination therapy in two cohorts. Five cytokine release syndrome events occurred with monotherapy, including one that met the criteria for dose-limiting toxicity at the highest dose; no other SYNB1891-related serious adverse events occurred, and no SYNB1891-related

Corresponding Author: Jason J. Luke, Immunotherapy and Drug Development Center, UPMC Hillman Cancer Center, Pittsburgh, PA 15232. Fax: 412-623-7948; lukejj@upmc.edu.

Authors' Contributions

J.J. Luke: Formal analysis, investigation, writing–original draft, writing–review and editing. **S.A. Piha-Paul:** Investigation, writing–review and editing. **T. Medina:** Investigation, writing–review and editing. **C.F. Verschraegen:** Investigation, writing– review and editing. **M. Varterasian:** Investigation, methodology, writing–review and editing. **A.M. Brennan:** Conceptualization, writing–review and editing. **R.J. Riese:** Conceptualization, supervision, writing–review and editing. **A. Sokolovska:** Conceptualization, supervision, writing–review and editing. **J. Strauss:** Investigation, writing–review and editing. **D.L. Hava:** Conceptualization, formal analysis, supervision, writing–original draft, writing–review and editing. **F. Janku:** Investigation, writing–review and editing.

Supplementary data for this article are available at Clinical Cancer Research Online (http://clincancerres.aacrjournals.org/).

infections were observed. SYNB1891 was not detected in the blood at 6 or 24 hours after the first intratumoral dose or in tumor tissue 7 days following the first dose. Treatment with SYNB1891 resulted in activation of the STING pathway and target engagement as assessed by upregulation of IFN-stimulated genes, chemokines/cytokines, and T-cell response genes in core biopsies obtained predose and 7 days following the third weekly dose. In addition, a dose-related increase in serum cytokines was observed, as well as stable disease in 4 participants refractory to prior PD-1/L1 antibodies.

Conclusions: Repeat intratumoral injection of SYNB1891 as monotherapy and in combination with atezolizumab was safe and well tolerated, and evidence of STING pathway target engagement was observed.

Introduction

Immunotherapy using checkpoint inhibition (CPI) has become a foundational component of standard therapy across an array of oncologic indications; however, most tumors fail to respond (1). Intratumoral immune cell infiltration has been correlated with response to CPI therapy, as study participants with greater tumor-infiltrating lymphocytes prior to therapy have exhibited higher response rates (2). Combination therapies seek to expand response rates by driving higher levels of immune cell infiltration into tumors, triggering antigen-presenting cell (APC) activation and promoting productive tumor-antigen presentation to effector T cells (2). Innate immune agonists, such as Toll-like receptor (TLR) agonists (3) and STimulator of INterferon Genes (STING) agonists (4) have thus become mechanisms of substantial translational and clinical interest in overcoming CPI resistance.

Microbial-based therapies emerged as a treatment option in human cancer in 1891 when Dr. William B. Coley began treating patients with living bacterial cultures after observing spontaneous regressions in those with streptococcal infections (5). Initial work with intratumoral injections of active bacteria (Coley toxin) resulted in anecdotal tumor responses, highlighting a link between cancer and type 1 IFNs (6–9). Type 1 IFN-related gene expression signatures have been directly correlated to T-cell infiltration in tumors (10) with subsequent work linking type 1 and IFNγ to the development of the T cell–inflamed tumor microenvironment (TME). This phenotype has been strongly linked to CPI response (11) and raised the hypothesis that conversion of non–T cell-inflamed into T cell–inflamed tumors could facilitate CPI treatment response (12).

Because the STING pathway is required in immune recognition and elimination of tumors through type 1 IFN (13), STING agonists provide a promising approach to elicit type 1 IFN production (14). Cyclic dinucleotides (CDN), like cyclic-di-AMP (CDA), are unique nucleic acids that function as signaling molecules in bacteria and have induced a STING-dependent type 1 IFN response intracellularly (15). While small-molecule STING agonists have indicated potent induction of antitumor immunity (16), “off target” activation of STING in effector T cells can lead to T-cell apoptosis (17) and impede the establishment of immunologic memory (18). To reduce nontargeted, systemic effects and improve “on-target” efficacy, new STING activation methodologies are essential.

SYNB1891 is a genetically modified strain of *Escherichia coli* Nissle 1917 (EcN), a probiotic strain of *E. coli* engineered to activate STING in the intratumoral environment (19). Under hypoxic conditions, SYNB1891 expresses DacA from *Listeria monocytogenes* to convert ATP to CDA, a potent STING agonist (Supplementary Fig. S1). Upon intratumoral administration, SYNB1891 is taken up by APCs, such as dendritic cells and macrophages, within the TME in which the intracellular release of CDA induced by SYNB1891 activates the STING pathway and leads to upregulation of type I IFNs. In addition, parallel pathways of innate immune activation are triggered by the bacterial chassis itself through pattern recognition receptors (PRR), such as endotoxin stimulation of TLR4, which results in the release of additional cytokines. The release of these proinflammatory cytokines, type I IFNs and activation of APCs subsequently initiates and promotes antitumor immunity and immune rejection of the tumor. Studies by Leventhal and colleagues in tumor-bearing mice demonstrated that intratumoral SYNB1891 produced CDA locally within the TME, leading to acute increases in tumoral levels of both IFNβ and proinflammatory cytokines that were correlated with dose-dependent antitumor activity and complete tumor regressions. These regressions led to the generation of long-term systemic immunity as evidenced by tumor rejections upon rechallenge in mice that had previously undergone complete regressions (19). While both EcN and SYNB1891 enhanced murine tumor regression relative to sham injection, SYNB1891 was associated with longer survival and greater induction of IFN-associated gene expression across multiple immune cell populations (19). SYNB1891 was also engineered with several biocontainment and safety features to target the production of CDA to the TME (Supplementary Fig. S1). The organism is sensitive to human serum and to antibiotics. As a result of two gene deletions, the organism lacks the ability to produce thymidine and cell wall diaminopimelic acid thus limiting the ability of the organism to proliferate in the absence of specific supplementation. Preclinical tests of SYNB1891 showed synthesis of CDA in the TME and confirmed the inability of the SYNB1891 to create a locally proliferative or blood borne infection in mice.

Escalating doses of intratumoral SYNB1891 with and without atezolizumab were investigated with the intent of establishing safety and STING target engagement. It was hypothesized that agonism of the STING pathway (and other PRRs) by SYNB1891 would result in productive T-cell priming and trafficking but sustained antitumor activity might require inhibition of the PD-1/PD-L1 pathway. Here we demonstrate that monotherapy and combination therapy can be safety delivered with an expected toxicity profile and observation of type I IFN-associated pharmacodynamics in tumor and peripheral blood.

Patients and Methods

A phase I open-label, multicenter, two-arm study was conducted between December 2019 and December 2021 with written informed consent of the study subjects and otherwise in accordance with the provisions of the Declaration of Helsinki and the International Conference on Harmonization Guidelines for Good Clinical Practice (NCT04167137). Study participants reviewed and signed informed consent forms approved by site-specific ethics committees prior to undergoing study-related procedures.

Study objectives were to evaluate the safety, tolerability, pharmacokinetics, pharmacodynamics, and preliminary efficacy of SYNB1891 when administered either as monotherapy (arm 1) or in combination with atezolizumab (arm 2) in participants with advanced/metastatic cancer.

In arm 1, participants received up to four 21-day cycles of SYNB1891 monotherapy. On days 1, 8, and 15 of cycle 1 and day 1 of cycles 2 through 4, participants received an intratumoral injection of SYNB1891 into an eligible lesion. The starting dose of SYNB1891 in the first cohort was 1×10^6 live cells and was increased in approximately 3-fold increments in subsequent cohorts until MTD determination in accordance with the modified toxicity probability interval (mTPI) algorithm (20). Cohorts of participants were enrolled to receive escalating doses of SYNB1891 administered by intratumoral injection until the target dose-limiting toxicity (DLT) range (~30%) for SYNB1891 monotherapy was determined on the basis of DLTs observed in cycle 1 (arm 1). The dose selected as achieving the target DLT range would be considered the MTD. Prespecified DLTs included, but were not limited to, certain treatment-related grade 3/4 laboratory values, sepsis, toxicity resulting in death, discontinuation of cycle 1, or delay of cycle 2. SYNB1891 injections were administered in the outpatient setting and participants were closely observed at the clinic for at least 6 hours postinjection. Participants were contacted by telephone on cycle 1 day 3 to monitor for signs of cytokine release syndrome (CRS).

In arm 2, participants received SYNB1891 on the same schedule as in arm 1. In addition, atezolizumab was administered in accordance with its recommended dose and schedule (1,200 mg i.v. every 3 weeks) onday1 ofeach of thefour planned cycles. On days when atezolizumab and SYNB1891 were both administered, SYNB1891 was administered first, followed by at least 1 hour of observation prior to the atezolizumab infusion. Arm 2 dosing began after participants in arm 1 cohort 4 (3×10^7 live cells) completed their cycle 1 DLT safety evaluation. The starting dose of intratumoral SYNB1891 in the first cohort of arm 2was at the SYNB1891 arm 1 cohort 3 dose level (1×10^7 live cells), with subsequent cohorts receiving increased SYNB1891 doses in approximately 3-fold increments until recommended phase II dose (RP2D) determination. SYNB1891 combination dosing in arm 2 was always at least one dose level below the SYNB1891 monotherapy dose being evaluated in arm 1, with combination doses not escalated above the SYNB1891 single-agent MTD established in arm 1.

After the initial four cycles of study treatment in either arm, participants without progressive disease may have received additional cycles of their assigned study treatment for up to 24 months (i.e., cycles 5 to 35) until documentation of progressive disease or other discontinuation criteria, satisfaction of a predefined study stopping rule, or no eligible lesions remained. Study participants were followed through 30 ± 5 days after the last dose of study treatment.

Eligibility

Eligible adult study participants had histologically or cytologically confirmed stage III/IV advanced/metastatic solid tumor or lymphoma for which no therapeutic options were available. Participants had ≥1 injectable, measurable lesion [≥10 mm in diameter (≥15 mm

for nodal)] in accordance with the appropriate scale for their disease type. Eligible lesions were not located in the thoracic cavity, spleen, pancreas, gastrointestinal tract (liver injection was allowed), or cranium, were amenable to percutaneous injection, and were away from major blood vessels or neurologic structures. Eligibility required an Eastern Cooperative Oncology Group performance status of 0–1, life expectancy ≥ 3 months, oxygen saturation > 90% without supplementation, adequate cardiac function, and laboratory values within protocol-specified ranges.

Participants must not have had diagnosed immunodeficiency, previous/concurrent malignancies, allergy to antibiotics used to treat *E. coli* infection, or grade 3 or higher infections within 28 days prior to initiation of study dosing. Restrictions on therapy given prior to initiation of study dosing included live vaccines within 90 days; systemic immunostimulatory agents or investigational products within 28 days or 5 drug elimination half-lives; chemotherapy, radiation, or biological cancer therapy within 14 days; and antibiotics or immunosuppressive medications (aside from replacement doses with prednisone ≤ 10 mg/day or equivalent) within 7 days. For participants whose injected tumors were visceral, long-acting antiplatelet agents or therapeutic doses of anticoagulants were also prohibited, aside from preventative low molecular weight heparin (21). Participants in arm 2 must have been eligible to receive atezolizumab per local prescribing information. Adequate contraception was required, and pregnant/lactating women were excluded.

Drug supply

SYNB1891 investigational drug product was formulated in buffer composed of 15% glycerol, 5%trehalose, and 10 mmol/L Trisat pH 7.5. The concentrated SYNB1891 drug product (1×10^{11} live cells/mL) was thawed and diluted to a volume of 5 mL in room temperature 5% dextrose in water for injection and held at room temperature while handling for no more than 2 hours from the time of thaw to the time of administration. Once the dilutions were prepared, 0.3 mL of the prepared cell concentration was withdrawn, changing the needle to the appropriate length for the tumor to be treated prior to injection, and local protocol was followed to obtain the final dose volume of 0.1 mL.

Atezolizumab was supplied by the manufacturer as a sterile liquid in single use 20-mL glass vials (1,200 mg/vial) and was prepared and administered in accordance with local prescribing information as an intravenous infusion at a dose of 1,200 mg every 3 weeks.

Efficacy and disease biomarker assessments

Disease status was assessed evaluating injected lesions versus non-injected lesions and overall RECIST (22) changes per investigator assessment every two cycles.

Biomarkers of SYNB1891 target engagement were assessed in formalin-fixed, paraffin-embedded tumor core biopsy blocks. Core biopsy samples were collected at baseline and then on day 22, after the first three doses with SYNB1891. Biopsies were analyzed by hematoxylin and eosin staining to determine tumor cell content and samples were chosen for analysis of gene expression by NanoString and immune cells by immunofluorescence. NanoString analysis was conducted on samples collected from the same tumor pre-

and post-SYNB1891 treatment using the nCounter PanCancer Immune Profiling Panel (NanoString).

Immune cell composition of baseline and injected tumors was assessed using a custom-designed immunofluorescence multiplex assay developed for the staining of CD4, CD8, CD11c, FoxP3, granzyme B, Ki67, MHC class II, and PDL1 (Ultivue). Collected images were analyzed using Indica Labs HALO image analysis software to determine the percent positivity of each marker and to assess coexpression of multiple markers.

SYNB1891 pharmacokinetics was assessed in blood and tumor samples by quantitative PCR. Blood was collected on during cycle 1 of SYNB1891 predose, 6 hours postdose and 24 hours postdose. Tumor levels of SYNB1891 were assessed in fine-needle aspirates predose in cycle 1 and on day 8, 7 days post-SYNB1891 dosing. The lower limit of quantification was 3.3×10^4 copies/mg and 2.7×10^3 copies/mL in blood and tumor samples, respectively.

Systemic markers of pharmacodynamic activity were assessed by measuring serum cytokine levels at baseline, 6 hours postdose and 24 hours postdose.

Mouse studies

Mouse studies using the B16.F10 melanoma were conducted as described previously (19). Briefly, B16.F10 melanoma (ATCC, CRL-6475) cells were cultured under standard conditions as specified by ATCC (37°C incubator, 5% CO_2, humidified) in recommended media. Cells were rinsed in Dulbecco's PBS (DPBS) twice to remove excess FBS and resuspended in DPBS for implantation. Mice were injected with 2×10^5 cells subcutaneously using a 26-gauge needle into the shaved, left or right flank and tumors were allowed to establish until they reached between 40 and 300 mm^3. Mice were then randomized into treatment groups based on tumor volume to create groups with approximately equal average tumor volumes. SYNB1891 (2.9×10^9 live cells) or saline (50 μL) were injected intratumorally into the largest section of the tumor and the slow, consistent release of contents. Six days after injection tumors were collected and processed to isolate total RNA using TurboCapture mRNA (Qiagen) following the manufacturer's instructions. NanoString analysis was conducted on SYNB1891 and vehicle treated samples to determine gene expression changes in IFN and IFN-stimulated genes.

Statistical methods

Safety analyses were performed on participants who received at least one dose of SYNB1891 or atezolizumab. Efficacy analyses were performed on treated participants with an on-treatment response assessment, including those who discontinued for progressive disease prior to the first scheduled response assessment. Adverse events (AE) were coded using the Medical Dictionary for Regulatory Activities (MedDRA), version 22.0, and the severity of AEs and laboratory abnormalities were graded using the NCI Common Terminology Criteria for Adverse Events, version 5.0 (US DHHS 2017).

Data availability

The data that support the findings of this study are available from the corresponding author, J.J. Luke, upon reasonable request.

Results

Thirty-two participants were enrolled, including 24 participants in arm 1 (monotherapy) and 8 participants in arm 2 (combination therapy; Supplementary Fig. S2). Four participants (13%) in arm 1 completed the initial four planned cycles of study treatment; all other participants (28 participants, 88%) discontinued prematurely for the following reasons: disease progression (17 participants, 53%), withdrawal of consent (5 participants, 16%), AEs (2 participants, 6%), physician decision (2 participants, 6%), death due to tracheal hemorrhage from squamous cell carcinoma (1 participant, 3%), and study termination by the Sponsor (1 participant, 3%).

Most participants were White (29 participants, 91%), female (20 participants, 63%), and < 65 years of age (21 participants, 66%). Study participants had received up to eight prior lines of systemic therapy, with the most common disease types of melanoma (8 participants, 25%), sarcoma (5 participants, 16%), and esophageal cancer (4 participants, 13%; Table 1).

Safety

SYNB1891 was administered as an intratumoral injection at a dose range of 1×10^6 to 3×10^8 live cells as monotherapy (part 1) and led to one study participant experiencing DLT [serious AE (SAE) of grade 3 CRS] at 3×10^8 live cells. In combination with atezolizumab (part 2), no DLTs were seen up to dose level 2 (3×10^8 live cells) though no further escalation was performed because of sponsor decision to terminate study. The maximum administered doses of SYNB1891 were deemed safe in both arms, with no MTD/RP2D determined for either arm.

Study participants received a median of 2.0 (range, 1–16) monotherapy cycles or 2.0 (range, 1–7) combination therapy cycles. No dose reductions occurred. Study dosing was held for 7 participants (22%), most of whom had one or two doses held for AEs (abdominal pain, COVID-19 infection, CRS, dyspnea, diarrhea, nausea, pyrexia, and vomiting). One participant in arm 1 permanently discontinued SYNB1891 because of the DLT/SAE of grade 3 CRS.

All study participants experienced at least one treatment-emergent AE (TEAE), with events occurring in > 20% of participants including chills (13 participants, 41%), pyrexia (9 participants, 28%), and nausea (7 participants, 22%; Table 2). The maximum severity of TEAEs were mostly grade 1 (7 participants, 22%), grade 2 (12 participants, 38%), and grade 3 (31%) Three participants (9%) experienced grade 5 events which were all not treatment related. Fourteen participants (44%) experienced TEAEs related to SYNB1891, most of which were mild to moderate in severity. Four participants (13%) experienced SAEs that were considered related to SYNB1891 treatment, all of which were events of CRS occurring in the monotherapy cohorts.

AEs of special interest

Five participants (16%), all in arm 1, experienced CRS, with CRS occurring after the first dose of SYNB1891 for 3 participants and after the second dose for 2 participants. One CRS event, occurring at the dose of 3×10^8 live cells, was assessed as grade 3, was associated with respiratory failure, met the criteria for DLT/SAE, and resulted in treatment discontinuation. Three of the remaining 4 participants were successfully able to continue treatment, and 1 participant stopped treatment for an unrelated reason. All injection site reactions were grade 1 or 2. These reactions were variably treated with supportive medications and prophylactic medications on subsequent cycles. Injection site reactions did not prohibit further dosing with SYNB1891. One participant (3%) had an SAE of grade 3 sepsis considered not related to study dosing given identification of different bacteria causing infection. No infections related to SYNB1891 were observed.

Cancer outcomes

Nine of 25 evaluable study participants (36%) experienced best response of stable disease (SD; Fig.1). The duration of SD ranged from 1 to 363+ days, with 4 participants experiencing SD for over 2 months; 3 patients receiving monotherapy and the fourth combination. These included 1 participant (arm 1, 1×10^6 live cells) with mucosal melanoma of the vulva who had SD for 227 days; 1 participant (arm 1, 3×10^6 live cells) with basal cell carcinoma had SD for 87 days; 1 participant (arm 1, 1×10^7 live cells) with small cell lung cancer (SCLC) who had SD for 363+ days and 1 participant (arm 2, 3×10^7 live cells + atezolizumab) with endometrial cancer had SD for 128 days. There were no particular molecular features (PD-L1, microsatellite instability, etc.) that stood out as likely factors predisposing for extended time on treatment; however, study participants with longer SD predominately had single sites of disease for injection. There was also no association between CRS and cancer outcome.

Pharmacodynamics

SYNB1891 was not detected in the blood at 6 or 24 hours after the first intratumoral dose nor in the tumor tissue 7 days following the first dose at any dose level up to 3×10^8 live cells. Increases in serum cytokines (TNFα, IL6, IFNγ, IL1RA) were observed at 6 or 24 hours after the first intratumoral dose (Fig. 2A–D). The greatest fold-increases from baseline values were observed in subjects receiving 1×10^7, 3×10^7, and 1×10^8 live cells of SYNB1891 (Supplementary Fig. S3), although no statistically significant differences between groups were observed, noting the small sample sizes of the groups. These changes did not associate with differential cancer outcomes.

To evaluate target engagement and STING activation by SYNB1891, mRNA analysis was performed on matched core biopsy pairs of injected tumors obtained predose and 7 days following the third weekly dose from 12 participants (10 participants in arm 1, 2 participants in arm 2; Supplementary Table S1). Assessment of SYNB1891 target engagement and STING activation focused on analysis of IFN and IFN-stimulated gene expression, and downstream pathways involved in antitumor immunity. To inform this analysis, the effect of SYNB1891 treatmenton IFN and IFN-stimulated gene expression in B16.F10 tumor-bearing mice was evaluated 6 days after treatment. Compared with vehicle-treated animals,

intratumoral injection of SYNB1891 (2×10^9 live cells) resulted in significant upregulation of an 11-gene IFN-stimulated gene panel (Supplementary Fig. S4). In similar studies, SYNB1891 treatment resulted in durable antitumor immune responses and dose-dependent increases in intratumoral chemokines and cytokines (19).

In humans, baseline gene expression patterns between different tumor types varied, with some tumors showing evidence of immune reactivity and others exhibiting low gene expression immune-related gene, evinced by low levels of T cell and antigen presentation mRNA levels in tumor biopsies (Fig. 3A). Tumor characteristics for the NanoString analysis are shown in Supplementary Table S1. Following dosing with SYNB1891, 10 of the 12 SYNB1891-treated tumors exhibited upregulation of multiple IFN-stimulated genes and/or type I IFN genes (defined as >1.5-fold increase in at least three genes), with several genes increased >3-fold compared with baseline values (Fig. 3B and C). Tumor samples from a chondrosarcoma of the bone (1e7 live cell dose; subject 100–005) and melanoma (1e8 live cell dose; subject 600–006) showed no induction of IFN response. In addition, eight tumors also showed engagement of the T-cell compartment as upregulation of T-cell markers and genes (defined as >1.5-fold increase in at least three genes) related to T-cell costimulation and checkpoint inhibition (Fig. 3D and E). Evidence of immune activation by the SYNB1891 chassis was evident through the upregulation of genes encoding chemokine and cytokines, as well as genes involved in TLR signaling and antigen presentation (Supplementary Figs. S5 and S6). Despite the gene upregulation in most tumors, the level of upregulation varied and was not clearly associated with tumor type or dose.

The two participants with the longest period of SD exhibited correlative increases in STING pathway activation and improved inflammatory responses. Subject 600–002 (1×10^7 live cells of SYNB1891) experienced SD for >363 days after injection of a SCLC nodal mass and subject 100–002 (1×10^6 live cells of SYNB1891) had SD for 227 days after injection of in-transit melanoma. In both participants, injected tumor diameters decreased by >10% over the first eight cycles of therapy (Fig. 4A and D). After cycle 1, both participants had evidence of STING activation, increased T-cell responses and increased inflammatory signaling within the TME by mRNA analysis (Fig. 4B and 4E). Enhanced T-cell recruitment and activation was also evident by multiplex immunofluorescence staining of core biopsy samples, which showed increases in $CD4^+$ and $Ki67^+CD4^+$ cells as well as a small increase in $CD8^+$ and $Ki67^+CD8^+$ cells after one cycle of dosing (Fig. 4C and F; Supplementary Fig. S7). Notably, these samples also had a significant percentage of $CD11c^+$ in the TME at baseline, which constitute a target cell type for SYNB1891 and STING agonism. In contrast, tumor core biopsy samples from subjects 200–003 and 100–005, both of whom experienced progressive disease, exhibited few $CD11c^+$ cells and $CD4^+/CD8^+$ T cells at baseline and no evidence of increases after treatment with SYNB1891 (Supplementary Figs. S7 and S8).

Discussion

In this open-label, multicenter, parallel dose-escalation phase I study, repeated intratumoral injection of SYNB1891, an engineered strain of EcN designed to express CDN, with or without atezolizumab, demonstrated feasibility with a manageable safety profile and confirmation of STING pathway engagement. On-target associated immune activation

(CRS) was a common, and easily manageable, AE. No infectious EcN-associated toxicities were observed. SYNB1891 was not detected in the blood at any time but was confirmed present in tumor with clearance within the first week. Target engagement of the STING pathway was confirmed by peripheral blood cytokines, as well as gene expression changes in tumor tissue. Time on treatment in multiple study participants was preliminarily associated with expected patterns for induction of the type I and II IFN pathways in the TME.

Cancer immunotherapy for solid tumors is characterized by infiltration of tumor-infiltrating lymphocytes, chemokine gradients associated with recruitment of APCs and effector T cells as well as upregulation of IFNγ-associated immune-evasion pathways (12). This TME phenotype has been described as T cell–inflamed and is generally associated with both high levels of PD-L1 and response to immune checkpoint inhibitors (ICI; ref. 23). Despite this, most patients with advanced solid tumors do not respond to ICI or eventually develop resistance.

A major unmet need in the field then is TME interventions that generate *de novo* immune responses in non–T cell–inflamed tumors or overcome resistance in T cell–inflamed tumors. Therapies triggering type I IFN responses in the TME have the potential to facilitate both of these issues. Of various PRRs regulating type I IFN, the induction of the T cell–inflamed TME and response to ICI has been linked directly to the cGAS/STING pathway across both murine and human biology (10). First-generation STING agonists have been reported demonstrating preliminary signals of clinical activity though these did not advance into later-stage clinical trials at least partially due to an unattractive clinical benefit to toxicity profile (24). A limitation of these therapies was the induction of CRS at higher doses and lack of clarity surrounding TME retention (intratumoral pharmacokinetic) upon injection. Here we have described an intratumoral STING agonist that is conditionally produced only in the anerobic environment of the TME.

A consideration surrounding this approach to STING agonism is the vehicle of delivery. Vectors ranging from virus to various bacterial species have been explored in cancer therapy (25), though only one virus-based medicine, TVEC, has advanced to FDA approval for cancer (26). SYNB1891 and the engineered EcN platform differentiates from these approaches in several advantageous ways. EcN has multiple useful features, including serum sensitivity in human blood (27), broad antibiotic sensitivity (28), as well as a defined genomic landscape for synthetic biologic engineering (29, 30). As a cancer therapeutic, some bacteria, particularly EcN, are ideal vectors in directly targeting STING agonism by phagocytosis into dendritic cells and other APCs (19). In addition, these vectors leverage an added benefit of triggering PRRs, notably including TLRs, which may further stimulate anticancer immunity. The component contribution of TLR4 agonism from EcN versus SYNB1891 has been previously elucidated in murine models (19). We observe that the incidence of CRS observed with SYNB1891 in this study appears promising relative to rates described for other PRR-based therapies; however, larger samples sizes would be necessary to conclude this.

An ongoing question in the field of cancer immunotherapy surrounds systemic efficacy associated with intratumoral delivery of immune-modifying cancer therapeutics. Preclinical

models have demonstrated major local and systemic antitumor effects of STING agonists. These models are hampered by greater baseline immuno-genicity than many human tumors due to syngeneic tumor implantation (31) and/or the presence of an engineered antigen (e.g., SIY; ref. 13). In clinical trials to date, results of intratumoral therapies have been mixed. Both the oncolytic virus TVEC and the CPG-B TLR9 agonist tilsotolimod failed to improved outcomes in randomized studies when combined with immune checkpoint inhibition (32). However, monotherapy with the intratumoral virus-like particle encapsulated CPG-A agonist vidutolimod has demonstrated an approximately 25% response rate in ICI refractory melanoma (33). In addition, preliminary evidence for intratumoral chemotherapy and other innate modifying approaches is emerging suggesting systemic immune modulation with intratumoral therapy (34).

As the impact on systemic disease from intratumoral therapy continues to be elucidated, a rising opportunity for application of intratumoral therapies may be in neoadjuvant therapy. Multiple clinical trials have now demonstrated that driving tumors to pathologic complete response before surgery strongly associates with event-free survival over time (35). STING agonism may be particularly well situated for this role in the perioperative setting given the strong rational for combination with irradiation, chemotherapy, and immunotherapy (36).

A limitation in the interpretation of our study is the enrollment of heavily pretreated patients with heterogeneous tumor histologies, which prevents predicting potential efficacy for a specific tumor type. However, the translational observations from our study could inform next steps to further explore individual diseases. Our study did not address the most appropriate (high vs. low) dose of STING agonism, an ongoing question in the field (18). Preclinical modeling of the STING agonist ADU-S100 suggested that high doses of STING agonism were deleterious to effector T cells. High doses did have a direct anticancer effect, via vascular collapse within the tumor, however, did not lead to systemic immune priming. Our dose-escalation study was only modestly sized; however, we observed that tumors demonstrated mechanism-consistent molecular changes at both lower and higher doses. Further exploration of optimal dosing for STING agonists may be a priority for the field but will not be possible with SYNB1891 as drug manufacture was discontinued after change in the study sponsor’s corporate focus away from oncology.

In summary, we have demonstrated that administration of intratumoral gene-modified EcN-expressing CDN, as monotherapy and with atezolizumab, is clinically feasible and demonstrates STING pathway target engagement. Intratumoral *E. coli* delivered STING agonism may have potential to enhance cancer immunotherapy in a diverse array of clinical settings.

Supplementary Material

Refer to Web version on PubMed Central for supplementary material.

Acknowledgments

The study and article development were funded by Synlogic Operating Company, Inc.

The authors would like to thank the study participants and their families, as well as investigational site personnel.

Authors' Disclosures

J.J. Luke reports DSMB participation with AbbVie, Agenus, Immutep, and Evaxion; scientific advisory board participation with (no stock): 7 Hills, Affivant, BioCytics, Bright Peak, Exo, Fstar, Inzen, RefleXion, and Xilio and (stock): Actym, Alphamab Oncology, Arch Oncology, Duke Street Bio, Kanaph, Mavu, NeoTx, Onc. AI, OncoNano, physIQ, Pyxis, Saros, STipe, and Tempest; consultancy with compensation from AbbVie, Agenus, Alnylam, AstraZeneca, Atomwise, Bayer, Bristol-Myers Squibb, Castle, Checkmate, Codiak, Crown, Cugene, Curadev, Day One, Eisai, EMD Serono, Endeavor, Flame, G1 Therapeutics, Genentech, Gilead, Glenmark, HotSpot, Kadmon, KSQ, Janssen, Ikena, Inzen, Immatics, Immunocore, Incyte, Instil, IO Biotech, Macrogenics, Merck, Mersana, Nektar, Novartis, Partner, Pfizer, Pioneering Medicines, PsiOxus, Regeneron, Replimmune, Ribon, Roivant, Servier, STINGthera, Synlogic, and Synthekine; research support (all to institution for clinical trials unless noted) from AbbVie, Astellas, AstraZeneca, Bristol Myers Squibb, Corvus, Day One, EMD Serono, Fstar, Genmab, Hot Spot, Ikena, Immatics, Incyte, Kadmon, KAHR, Macrogenics, Merck, Moderna, Nektar, Next Cure, Numab, Palleon, Pfizer, Replimmune, Rubius, Servier, Scholar Rock, Synlogic, Takeda, Trishula, Tizona, and Xencor; and patents (both provisional) Serial #15/612,657 (Cancer Immunotherapy) and PCT/US18/36052 (Microbiome Biomarkers for Anti-PD-1/PD-L1 Responsiveness: Diagnostic, Prognostic and Therapeutic Uses Thereof). S.A. Piha-Paul reports other support from AbbVie, ABM Therapeutics, Acepodia, Alkermes, Aminex Therapeutics, Amphivena Therapeutics, BioMarin Pharmaceutical, Boehringer Ingelheim, Bristol Myers Squibb, Cerulean Pharma, Chugai Pharmaceutical Co., Ltd, Curis, Cyclacel Pharmaceuticals, Daiichi Sankyo; Eli Lilly, ENB Therapeutics, Epigenetix Inc., Five Prime Therapeutics, F-Star Beta Limited, F-Star Therapeutics, Gene Quantum, Genmab A/S, Gilead Sciences, GlaxoSmithKline, Helix BioPharma Corp., Hengrui Pharmaceuticals Co., Ltd., HiberCell, Immorna Biotherapeutics, Immunomedics, Incyte Corp., Jacobio Pharmaceuticals Co., Ltd., Jiangsu Simcere Pharmaceutical Co., Ltd., Lytix Biopharma AS, Medimmune, LLC, Medivation, Merck Sharp and Dohme Corp., Nectin Therapeutics, Ltd., Novartis Pharmaceuticals, Pieris Pharmaceuticals, Pfizer, Phanes Therapeutics, Principia Biopharma, Puma Biotechnology, Purinomia Biotech, Rapt Therapeutics, Replimune, Seattle Genetics, Silverback Therapeutics, Synlogic Therapeutics, Taiho Oncology, Tesaro, TransThera Bio, and ZielBio and grants from NCI/NIH, P30CA016672 – Core Grant (CCSG Shared Resources) outside the submitted work; in addition, S.A. Piha-Paul has worked as a consultant for CRC Oncology. T. Medina reports institutional funding from Synlogic, Merck, BMS, Genentech, Moderna, Regeneron, Replimune, Ultimovacs, InflaRx, Day One, Anaveon, Agenus, BioAtla, Trisalus, Seattle Genetics, Iovance, and Pfizer. A.M. Brennan reports other support from Synlogic during the conduct of the study. A. Sokolovska reports other support from Synlogic during the conduct of the study; in addition, A. Sokolovska has a patent for US20220023358A1 pending. J. Strauss reports personal fees from Mary Crowley Cancer Research during the conduct of the study as well as personal fees from Dialectic Therapeutics outside the submitted work; in addition, J. Strauss reports ownership of common stock in the following publicly traded pharmaceutical companies: AbbVie, Bristol-Myers Squibb, Intuitive Surgical, Johnson & Johnson, Merck, and Regeneron. D.L. Hava reports nonfinancial support and other support from Synlogic during the conduct of the study. F. Janku reports grants and personal fees from Synlogic during the conduct of the study as well as grants and personal fees from Asana Biosciences, Bicara, Deciphera, Fore Bio, Ideaya Biosciences, Novartis, PureTech Health, and Sotio; grants from Astex, BioMed Valley Discoveries, BioXcel, Bristol Myers Squibb, F-star, FujiFilm Pharmaceuticals, Hutchison Medipharma, Lilly, Merck, NextCure, and Sanofi; other support from Monte Rosa Therapeutics; personal fees from Crown Bioscience, Pega One, Flame Biosciences, Immunomet, Mersana Therapeutics, and MedinCell; and personal fees and other support from Cardiff Oncology outside the submitted work. No disclosures were reported by the other authors..

References

1. Darvin P, Toor SM, Sasidharan Nair V, Elkord E. Immune checkpoint inhibitors: recent progress and potential biomarkers. Exp Mol Med 2018;50:1–11.
2. Zou W, Wolchok JD, Chen L. PD-L1 (B7-H1) and PD-1 pathway blockade for cancer therapy: mechanisms, response biomarkers, and combinations. Sci Transl Med 2016;8:328rv4.
3. Karapetyan L, Luke JJ, Davar D. Toll-like receptor 9 agonists in cancer. Onco Targets Ther 2020;13:10039–60. [PubMed: 33116588]
4. Amouzegar A, Chelvanambi M, Filderman JN, Storkus WJ, Luke JJ. STING agonists as cancer therapeutics. Cancers 2021;13:2695. [PubMed: 34070756]
5. McCarthy EF. The toxins of William B. Coley and the treatment of bone and soft-tissue sarcomas. Iowa Orthop J 2006;26:154–8. [PubMed: 16789469]
6. Isaacs A, Lindenmann J. Pillars Article: Virus Interference. I. The interferon. Proc R Soc Lond B Biol Sci. 1957. 147: 258–267. J Immunol 2015;195:1911–20. [PubMed: 26297790]
7. Ivashkiv LB, Donlin LT. Regulation of type I interferon responses. Nat Rev Immunol 2014;14:36–49. [PubMed: 24362405]

8. Roberts NJ, Zhang L, Janku F, Collins A, Bai RY, Staedtke V, et al. Intratumoral injection of *Clostridium novyi*-NT spores induces antitumor responses. Sci Transl Med 2014;6:249ra111.
9. Janku F, Zhang HH, Pezeshki A, Goel S, Murthy R, Wang-Gillam A, et al. Intratumoral injection of *Clostridium novyi*-NT spores in patients with treatment-refractory advanced solid tumors. Clin Cancer Res 2021;27:96–106. [PubMed: 33046513]
10. Harlin H, Meng Y, Peterson AC, Zha Y, Tretiakova M, Slingluff C, et al. Chemokine expression in melanoma metastases associated with CD8+ T-cell recruitment. Cancer Res 2009;69:3077–85. [PubMed: 19293190]
11. Cristescu R, Mogg R, Ayers M, Albright A, Murphy E, Yearley J, et al. Pan-tumor genomic biomarkers for PD-1 checkpoint blockade-based immunotherapy. Science 2018;362:eaar3593. [PubMed: 30309915]
12. Trujillo JA, Sweis RF, Bao R, Luke JJ. T cell-inflamed versus non-T cell-inflamed tumors: a conceptual framework for cancer immunotherapy drug development and combination therapy selection. Cancer Immunol Res 2018;6:990–1000. [PubMed: 30181337]
13. Woo SR, Fuertes MB, Corrales L, Spranger S, Furdyna MJ, Leung MY, et al. STING-dependent cytosolic DNA sensing mediates innate immune recognition of immunogenic tumors. Immunity 2014;41:830–42. [PubMed: 25517615]
14. Ishikawa H, Barber GN. STING is an endoplasmic reticulum adaptor that facilitates innate immune signalling. Nature 2008;455:674–8. [PubMed: 18724357]
15. Corrales L, Glickman LH, McWhirter SM, Kanne DB, Sivick KE, Katibah GE, et al. Direct activation of STING in the tumor microenvironment leads to potent and systemic tumor regression and immunity. Cell Rep 2015;11:1018–30. [PubMed: 25959818]
16. Flood BA, Higgs EF, Li S, Luke JJ, Gajewski TF. STING pathway agonism as a cancer therapeutic. Immunol Rev 2019;290:24–38. [PubMed: 31355488]
17. Larkin B, Ilyukha V, Sorokin M, Buzdin A, Vannier E, Poltorak A. Cutting edge: activation of STING in T cells induces Type I IFN responses and cell death. J Immunol 2017;199:397–402. [PubMed: 28615418]
18. Sivick KE, Desbien AL, Glickman LH, Reiner GL, Corrales L, Surh NH, et al. Magnitude of therapeutic STING activation determines CD8. Cell Rep 2019;29:785–9. [PubMed: 31618645]
19. Leventhal DS, Sokolovska A, Li N, Plescia C, Kolodziej SA, Gallant CW, et al. Immunotherapy with engineered bacteria by targeting the STING pathway for anti-tumor immunity. Nat Commun 2020;11:2739. [PubMed: 32483165]
20. Ji Y, Wang SJ. Modified toxicity probability interval design: a safer and more reliable method than the 3 + 3 design for practical phase I trials. J Clin Oncol 2013;31:1785–91. [PubMed: 23569307]
21. Marabelle A, Andtbacka R, Harrington K, Melero I, Leidner R, de Baere T, et al. Starting the fight in the tumor: expert recommendations for the development of human intratumoral immunotherapy (HIT-IT). Ann Oncol 2018;29:2163–74. [PubMed: 30295695]
22. Eisenhauer EA, Therasse P, Bogaerts J, Schwartz LH, Sargent D, Ford R, et al. New response evaluation criteria in solid tumours: revised RECIST guideline (version 1.1). Eur J Cancer 2009;45:228–47. [PubMed: 19097774]
23. Ayers M, Lunceford J, Nebozhyn M, Murphy E, Loboda A, Kaufman DR, et al. IFN-γ-related mRNA profile predicts clinical response to PD-1 blockade. J Clin Invest 2017;127:2930–40. [PubMed: 28650338]
24. Meric-Bernstam F, Sweis RF, Hodi FS, Messersmith WA, Andtbacka RHI, Ingham M, et al. Phase I dose-escalation trial of MIW815 (ADU-S100), an intratumoral STING agonist, in patients with advanced/metastatic solid tumors or lymphomas. Clin Cancer Res 2022;28:677–88. [PubMed: 34716197]
25. Toso JF, Gill VJ, Hwu P, Marincola FM, Restifo NP, Schwartzentruber DJ, et al. Phase I study of the intravenous administration of attenuated Salmonella typhimurium to patients with metastatic melanoma. J Clin Oncol 2002;20:142–52. [PubMed: 11773163]
26. Andtbacka RH, Kaufman HL, Collichio F, Amatruda T, Senzer N, Chesney J, et al. Talimogene laherparepvec improves durable response rate in patients with advanced melanoma. J Clin Oncol 2015;33:2780–8. [PubMed: 26014293]

27. Grozdanov L, Zähringer U, Blum-Oehler G, Brade L, Henne A, Knirel YA, et al. A single nucleotide exchange in the wzy gene is responsible for the semirough O6 lipopolysaccharide phenotype and serum sensitivity of *Escherichia coli* strain Nissle 1917. J Bacteriol 2002;184:5912–25. [PubMed: 12374825]

28. Sonnenborn U, Schulze J. The non-pathogenic Escherichia coli strain nissle 1917 – features of a versatile probiotic. Microb Ecol Health Dis 2009;21:122–58.

29. Gurbatri CR, Lia I, Vincent R, Coker C, Castro S, Treuting PM, et al. Engineered probiotics for local tumor delivery of checkpoint blockade nanobodies. Sci Transl Med 2020;12:eaax0876. [PubMed: 32051224]

30. Charbonneau MR, Isabella VM, Li N, Kurtz CB. Developing a new class of engineered live bacterial therapeutics to treat human diseases. Nat Commun 2020;11:1738. [PubMed: 32269218]

31. Bibby MC. Orthotopic models of cancer for preclinical drug evaluation: advantages and disadvantages. Eur J Cancer 2004;40:852–7. [PubMed: 15120041]

32. Chesney JA, Ribas A, Long GV, Kirkwood JM, Dummer R, Puzanov I, et al. Randomized, double-blind, placebo-controlled, global Phase III trial of talimogene laherparepvec combined with pembrolizumab for advanced melanoma. J Clin Oncol 2022;41:528–40. [PubMed: 35998300]

33. Ribas A, Medina T, Kirkwood JM, Zakharia Y, Gonzalez R, Davar D, et al. Overcoming PD-1 blockade resistance with CpG-A Toll-like receptor 9 agonist vidutolimod in patients with metastatic melanoma. Cancer Discov 2021;11:2998–3007. [PubMed: 34326162]

34. Thomas JS, El-Khoueiry AB, Olszanski AJ, Azad NS, Whalen GF, Hanna DL, et al. Effect of intratumoral INT230–6 on tumor necrosis and promotion of a systemic immune response: results from a multicenter phase 1/2 study of solid tumors with and without pembrolizumab (PEM) [Intensity IT-01; Merck KEYNOTE-A10]. J Clin Oncol 40: 16s, 2022 (suppl; abstr 2520).

35. Forde PM, Spicer J, Lu S, Provencio M, Mitsudomi T, Awad MM, et al. Neoadjuvant nivolumab plus chemotherapy in resectable lung cancer. N Engl J Med 2022;386:1973–85. [PubMed: 35403841]

36. Deng L, Liang H, Xu M, Yang X, Burnette B, Arina A, et al. STING-dependent cytosolic dna sensing promotes radiation-induced type i interferon-dependent antitumor immunity in immunogenic tumors. Immunity 2014;41:843–52. [PubMed: 25517616]

Translational Relevance

The intracellular DNA sensor STimulator of INterferon Genes (STING) is a high-priority cancer immunotherapy target given roles in regulating type I IFN, antitumor activity demonstrated by STING agonists across preclinical models, and potential for out of injected field immune responses. Initial studies pursuing intratumoral injection of STING agonists may have been hampered by limited tumor microenvironment drug retention. To address this, the *Escherichia coli* Nissle 1917 was engineered to produce cyclic dinucleotides under conditions of hypoxia that may enhance STING activation within the tumor microenvironment after uptake by phagocytic antigen-presenting cells. We performed a dose-escalation study of the live probiotic SYNB1891, as an intratumor injected monotherapy and in combination with atezolizumab. We demonstrate local and systemic safety of this approach. Immune profiling of peripheral blood and tumor biopsies demonstrated STING pathway target engagement, as assessed by upregulation of IFN-stimulated genes, chemokines/cytokines, and T-cell response genes, as associated with time on treatment.

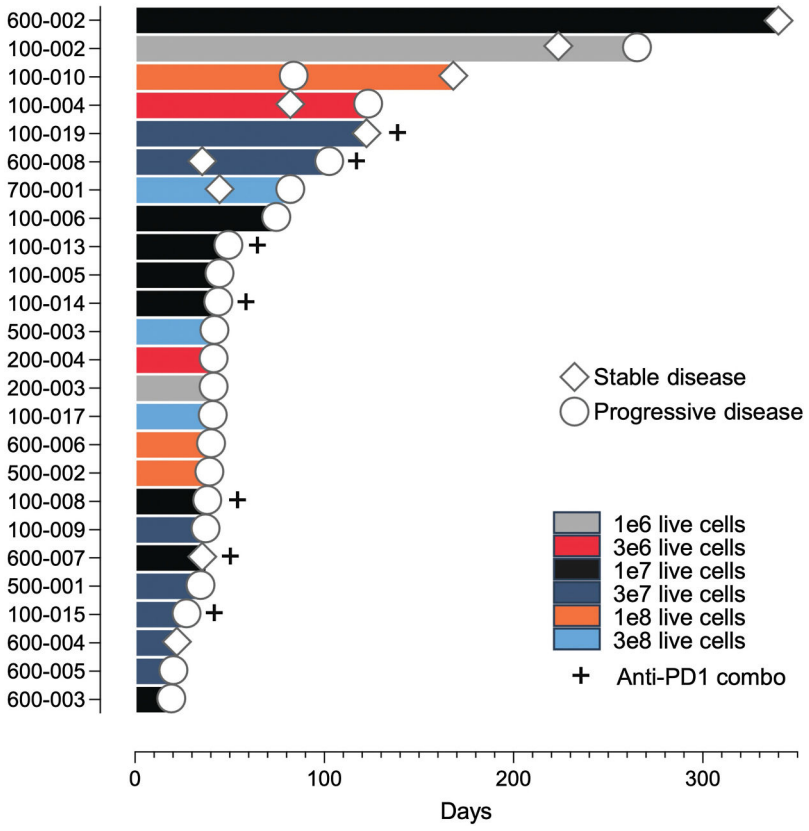

Figure 1.

Tumor response by RECIST. The best overall tumor response for each subject is shown. Colors indicate different dose levels of SYNB1891 and (+) denote subjects that received SYNB1891 and atezolizumab. SD (diamonds) and progressive disease (circles) are indicated.

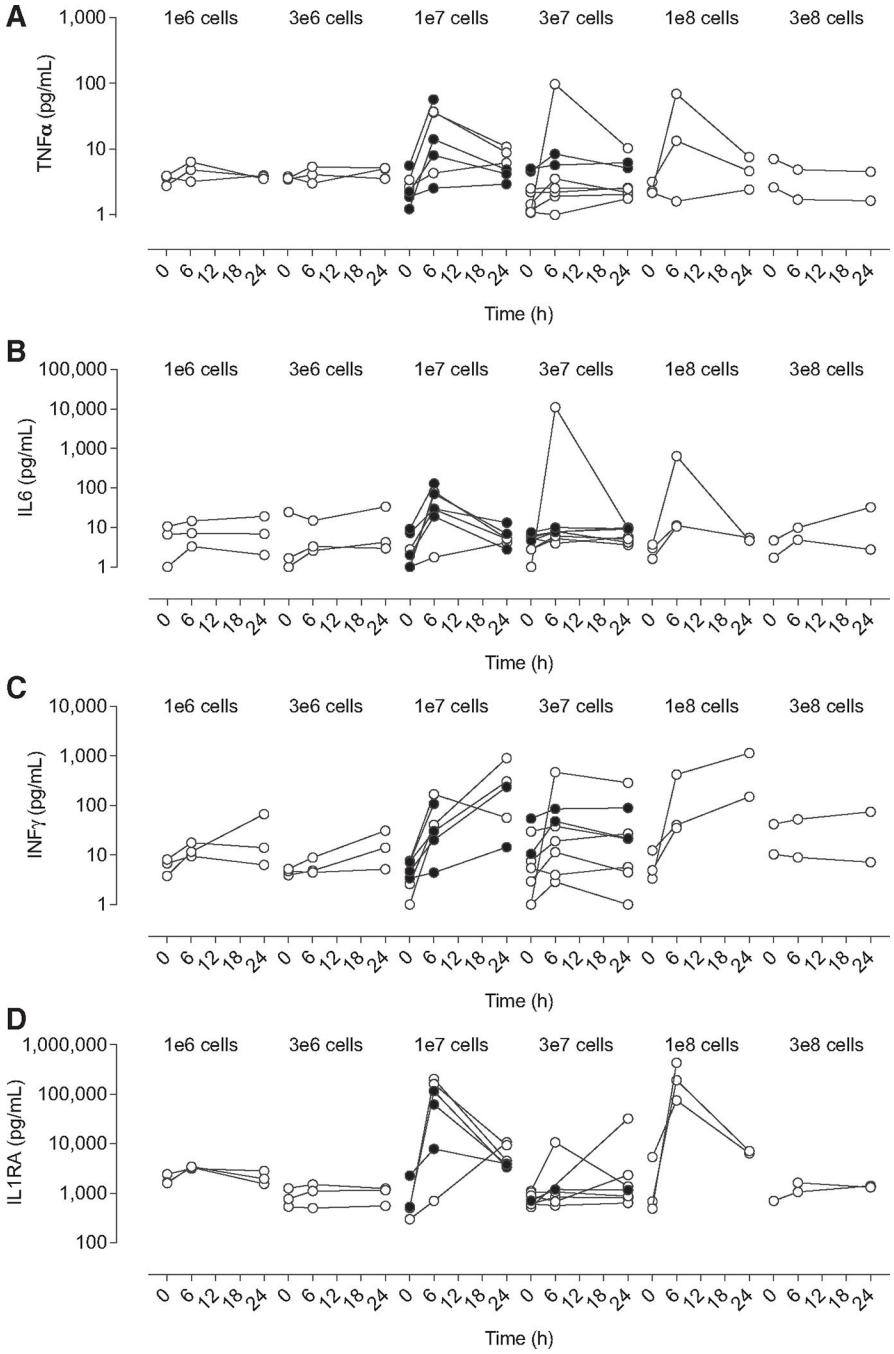

Figure 2.

Serum cytokine levels in subjects receiving SYNB1891. Levels of TNFα (**A**), IL6 (**B**), INFγ (**C**), and IL1RA (**D**) were measured at baseline (predose) and 6 and 24 hours after injection with increasing doses of SYNB1891. Open circles denote subjects receiving SYNB1891 and closed circles indicate subjects that received SYNB1891 and atezolizumab.

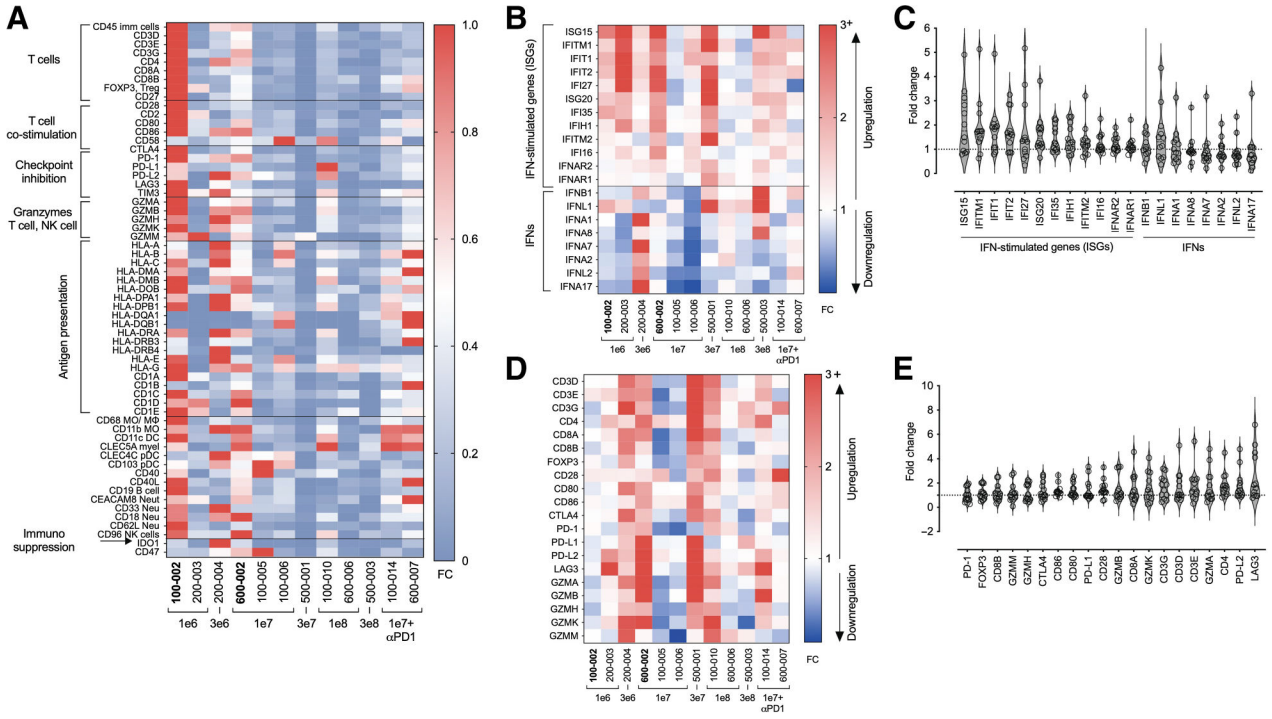

Figure 3.

Gene expression changes in tumors. Gene expression changes were assessed by NanoString in core biopsy samples collected predose and on day 22, 7 days after the last dose of cycle 1. **A**, Baseline tumor characteristics. Data were normalized to the highest and lowest expressed gene in each row, and each column represents a tumor sample from a subject receiving SYNB1891. Subject numbers and the dose of SYNB1891 administered are indicated on the *x*-axis. Two subjects with SD for > 2 months are indicated in bold. Tumor types for each analysis are presented in Supplementary Table S1. **B** and **C**, Fold changes in gene expression over baseline in injected tumors for IFN pathways and IFN responsive genes. **B**, Fold change in each gene relative to baseline are shown for patients receiving different doses of SYNB1891 labeled as described in **A**. **C**, Fold changes for each marker with each symbol representing the data from a single patient. **D** and **E**, Fold changes in gene expression over baseline in injected tumors for genes involved in T-cell responses. **D**, Fold changes in each gene relative to baseline are shown for patients receiving different doses of SYNB1891 label as described in **A**. **E**, Fold changes for each marker with each symbol representing the data from a single patient.

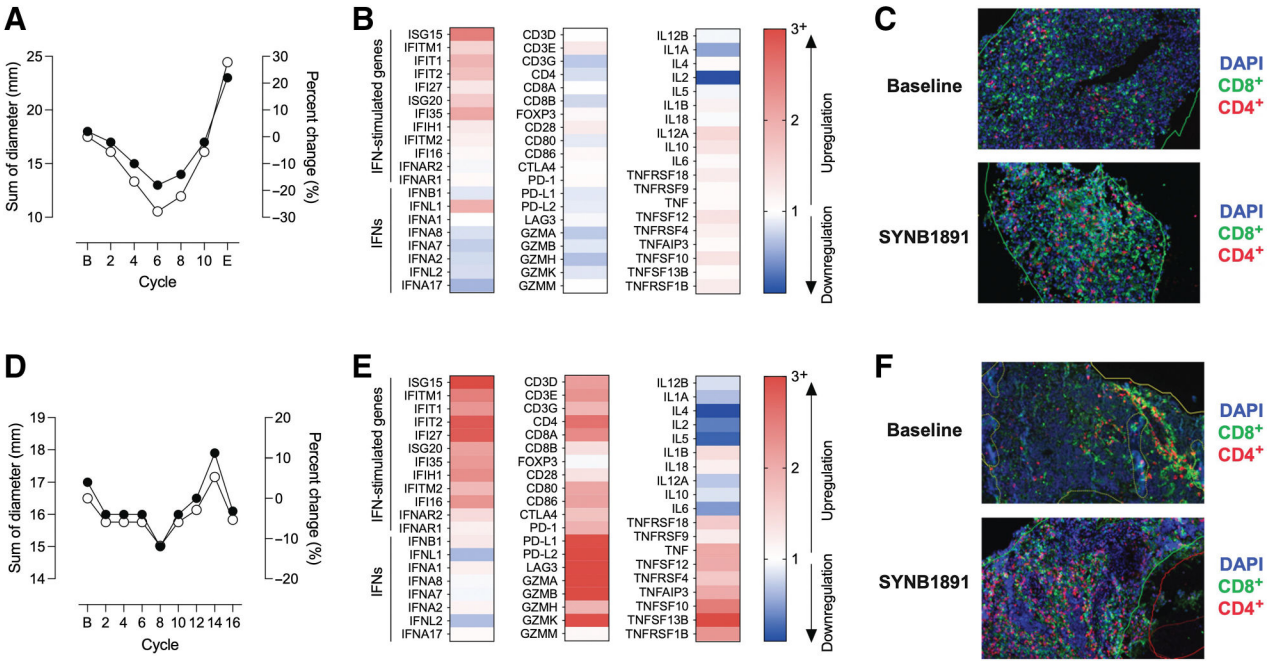

Figure 4.

Subjects with durable, SD have evidence of interferon pathway activation and increased T-cell recruitment to tumors. Data are shown for subjects 600–002 (**A**, **B**, and **C**) and 100–002 (**D**, **E**, and **F**). **A** and **D**, Changes in tumor size of injected lesions over time, with closed circles as sum of diameters and open circles as percent change. **B** and **E**, Fold changes in gene expression over baseline in injected tumors for IFN genes, T-cell–related genes and cytokine-related genes. **C** and **F**, Multiplex immunofluorescence staining of tumor core biopsies at baseline and after one cycle of SYNB1891 treatment.

Table 1.

Study participant characteristics (safety population).

Number of study participants treated		**Arm 1 (*N* = 24)**	**Arm 2 (*N* = 8)**
Age (years)	Median	61.5	60.5
	Range	25–82	37–77
Sex, *n* (%)	Male	7 (29)	5 (63)
	Female	17 (71)	3 (38)
Race, *n* (%)	White	21 (88)	8 (100)
	Black or African American	3 (13)	0
Hematology and clinical chemistry (median and range)	Hemoglobin	11.8 (9.1–15.2)	12.2 (10.2–13.3)
	Lymphocytes ($\times 10^9$/L)	1.2 (0.4–3.1)	1 (0.6–1.3)
	Neutrophil: lymphocyte	3.8 (1.1–13.8)	3.7 (2.0–9.7)
	Albumin (g/dL)	4.0 (3.2–4.9)	4.0 (3.1–4.8)
	Lactate dehydrogenase (U/L)	194 (119–1,232)	172 (154–1,299)
Prior systemic anticancer therapy (number of lines)	Median	3.0	3.5
	Range	1 to 8	2 to 7
Prior anticancer therapy, *n* (%)	Chemotherapy	18 (75)	7 (88)
	Immunotherapy	17 (71)	5 (63)
	Hormonal therapy	1 (4)	0
	Biological therapy	2 (8)	1 (13)
	Other	2 (8)	0
Disease, *n* (%)	Melanoma	7 (29)	1 (13)
	Sarcoma	5 (21)	0
	Esophageal cancer	1 (4)	3 (38)
	Other[a]	11 (46)	4 (50)
Number of RECIST target lesions at baseline	Median	4	3
	Range	1 to 5	2 to 4

[a] Includes 2 participants with oropharynx squamous cell carcinoma and 1 participant with each of the following: ampullary bile duct adenocarcinoma, basal cell carcinoma, cecum adenocarcinoma, colorectal cancer, endometrial cancer, jejunum adenocarcinoma, Merkel cell carcinoma, non–small cell lung cancer, rectosigmoid adenocarcinoma, skin squamous cell carcinoma, small cell lung cancer, testicular cancer, and vulvar squamous cell carcinoma.

Table 2.

TEAEs in ≥ 10% of participants (safety population).

	Arm 1							Arm 2			
Preferred term	**Cohort 1 1 × 10^6 cells (*N* = 3)**	**Cohort 2 3 × 10^6 cells (*N* = 3)**	**Cohort 3 1 × 10^7 cells (*N* = 4)**	**Cohort 4 3 × 10^7 cells (*N* = 5)**	**Cohort 5 1 × 10^8 cells (*N* = 3)**	**Cohort 6 3 × 10^8 cells (*N* = 6)**	**Total Arm 1 (*N* = 24)**	**Cohort 1 1 × 10^7 cells þ 1,200 mg (*N* = 4)**	**Cohort 2 3 × 10^7 cells þ 1,200 mg (*N* = 4)**	**Total Arm 2 (*N* = 8)**	**All participants (*N* = 32)**
Any TEAE, *n* (%)	3 (100)	3 (100)	4 (100)	5 (100)	3 (100)	6 (100)	24 (100)	4 (100)	4 (100)	8 (100)	32 (100)
Chills	1 (33)	1 (33)	0	1 (20)	2 (67)	4 (67)	9 (38)	2 (50)	2 (50)	4 (50)	13 (41)
Pyrexia	0	0	2 (50)	2 (40)	1 (33)	1 (17)	6 (25)	2 (50)	1 (25)	3 (38)	9 (28)
Nausea	1 (33)	0	1 (25)	1 (20)	3 (100)	1 (17)	7 (29)	0	0	0	7 (22)
Back pain	0	0	1 (25)	2 (40)	1 (33)	0	4 (17)	1 (25)	1 (25)	2 (25)	6 (19)
Headache	0	1 (33)	0	1 (20)	1 (33)	1 (17)	4 (17)	1 (25)	1 (25)	2 (25)	6 (19)
CRS	0	0	0	2 (40)	0	3 (50)	5 (21)	0	0	0	5 (16)
Fatigue	0	0	0	1 (20)	1 (33)	2 (33)	4 (17)	0	1 (25)	1 (13)	5 (16)
Hyponatraemia	0	0	3 (75)	0	2 (67)	0	5 (21)	0	0	0	5 (16)
Anemia	0	1 (33)	0	1 (20)	1 (33)	0	3 (13)	1 (25)	0	1 (13)	4 (13)
Constipation	0	1 (33)	1 (25)	0	0	2 (33)	4 (17)	0	0	0	4 (13)
Decreased appetite	0	1 (33)	1 (25)	0	0	0	2 (8)	2 (50)	0	2 (25)	4 (13)
Injection site pain	0	0	0	1 (20)	0	0	1 (4)	2 (50)	1 (25)	3 (38)	4 (13)
Vomiting	0	0	1 (25)	0	2 (67)	0	3 (13)	1 (25)	0	1 (13)	4 (13)

Note: Events in table are regardless of relationship to study agents.

Abbreviations: CRS, cytokine release syndrome; MedDRA, Medical Dictionary for Regulatory Activities; TEAE, treatment-emergent adverse event.